PAPER

Tunable plasmonic resonance arising from broken-symmetric silver nanobeads with dielectric cores

IOP PUBLISHING JOURNAL OF OPTICS
J. Opt. **14** (2012) 114010 (6pp) doi:10.1088/2040-8978/14/11/114010

Tunable plasmonic resonance arising from broken-symmetric silver nanobeads with dielectric cores

You Zhe Ho[1], Wei Ting Chen[2], Yao-Wei Huang[2], Pin Chieh Wu[2], Ming Lun Tseng[2], Yao Ting Wang[1], Yuan-Fong Chau[3] and Din Ping Tsai[1,2,4]

[1] Department of Physics, National Taiwan University, Taipei 10617, Taiwan
[2] Graduate Institute of Applied Physics, National Taiwan University, Taipei 10617, Taiwan
[3] Department of Electronic Engineering, Chien Hsin University of Science and Technology, Jung-Li 32095, Taiwan
[4] Research Center for Applied Sciences, Academia Sinica, Taipei 11529, Taiwan

E-mail: dptsai@phys.ntu.edu.tw

Received 23 February 2012, accepted for publication 26 July 2012
Published 26 September 2012
Online at stacks.iop.org/JOpt/14/114010

Abstract
We investigate the plasmonic resonance modes and coupling effects of single silver nanobeads and silver nanobead dimers. Numerical investigation using the three-dimensional finite element method indicates that silver nanobeads exhibit two plasmonic resonances corresponding to the bonding and anti-bonding modes, respectively. The boundary symmetry on the inner and outer surfaces of the silver nanobeads can be broken by increasing the refractive indices of the cores filling the dielectric holes. It is shown that only the bonding mode can be found for low-refractive index cores, whereas both bonding and anti-bonding modes can be found for high-refractive index cores.

Keywords: surface plasmon, plasmonics, tunable, nanobead, bonding mode, coupling

(Some figures may appear in colour only in the online journal)

1. Introduction

Noble metal nanoparticles, e.g. gold or silver, have been widely used in scientific and technological applications such as chemical biosensing [1, 2], spasers (i.e. quantum amplifiers of surface plasmons by stimulated emission of radiation) [3–5], data storage [6] and nanoscale optical spectrum manipulation [7, 8]. The near field optical properties of a single noble metal nanoparticle are governed by the interactions of free electrons of the nanostructures in resonance with the incident light [9], also known as localized surface plasmon resonance (LSPR) [10–13]. The enhanced localized field can be several orders of magnitude higher than that of the incident field. The optical response and the resonant frequency of LSPR of metal nanoparticles can be tuned by controlling their size, shape, and environment, which provides a starting point for emerging research fields like surface plasmon-based photonics or plasmonics [14–17].

A large two-photon luminescence efficiency for gold nanorods was observed in the scattering spectra [18]. Several numerical studies of this phenomenon have been performed on different particle shapes [19] and particles surrounded by shells [20]. However, the effects of silver nanobeads and silver nanobead dimer systems have not yet been considered or investigated.

In this paper, we numerically investigate the optical spectra and the plasmon resonances of silver nanobeads and silver nanobead dimers which have three different media filling the dielectric holes by using the three-dimensional finite element method (3D FEM). The enclosure of a single

silver nanobead and a nanobead dimer with dielectric holes forms open cavity models and the electromagnetic field is effectively confined in the gap of the nanobead dimer to generate high local field enhancement. We compared the optical response in the near field zone of a single nanobead and a nanobead dimer. The influences of wavelength of the incident light, the medium filling the dielectric holes, and the effects of core refractive index on 'bonding' and 'anti-bonding' modes are discussed in our simulations.

2. Simulation models, method and discussion

A single silver nanobead can be formed from a silver nanosphere with a cylindrical dielectric hole filling the central part of the silver nanosphere. Figures 1(a) and (b) show schematic diagrams of a silver nanobead and a silver nanobead dimer embedded in a vacuum, illuminated with a transverse magnetic (TM) plane wave in the wavelength range of $350 \leqq \lambda \leqq 1050$ nm. The cylindrical hole is filled with different media inside the hollow, the dielectric constants of which are chosen as $\varepsilon = 1$, 3 and 6.25, respectively. In this work, the radius of a silver nanobead d, the radius of the cylindrical dielectric hole R, the period of a unit cell P, and the gap distance D are set to be 50 nm, 25 nm, 400 nm and 25 nm, respectively. The dielectric function of silver is described by the Drude–Lorentz model [21].

In our simulations, we use 3D FEM (a commercial finite element solver, COMSOL Multiphysics 3.5a), with triangular high-order edge elements. To model the infinite simulation region with a 3D finite-geometry model we use anisotropic perfectly matched layers (PML) to avoid the reflective fields from the boundary of the computational domain.

3. Results and discussion

Here we report a new hybrid nanoparticle geometry that combines the plasmonic properties of both a dielectric core and nanoshells in a single structure. This dielectric core–metallic shell spheroid nanoparticle bears a remarkable resemblance to a bead, inspiring the name 'nanobead'. A nanobead is composed of a cylindrical core coated with a continuous nanometer-thick silver shell. Our proposed structure depicted in figure 1 is an open system formed by a nanoshell and a dielectric core. This structure possesses two tunable resonances arising from the hybridization [22] of the plasmons on the inner surface of the shell with the plasmons on the outer shell surface, and can be tuned by varying the medium filling the dielectric hole. The geometrically and materially sensitive hybrid plasmon resonances of the nanoshell with a dielectric core are rigorous mesoscopic analogues of the hybridized electronic wavefunctions of simple atoms and molecules. Thus, the two plasmon resonances of a nanoshell are denoted by the 'bonding' and 'anti-bonding' plasmonic modes, in direct analogy with molecular orbital theory [22].

Firstly, we investigate the difference in the transmittance spectra of an array of silver nanobeads with three different

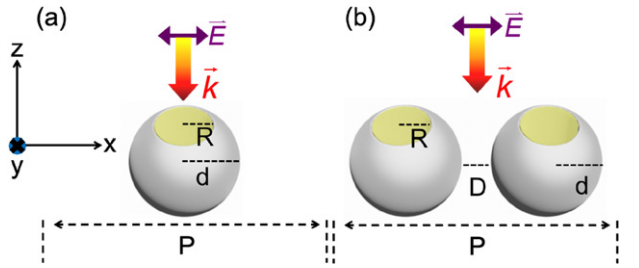

Figure 1. Schematic diagram of the simulation models: (a) a unit cell of a silver nanobead and (b) a silver nanobead dimer, with a cylindrical dielectric hole inside the central part of a silver nanosphere.

media (with $\varepsilon = 1$, 3 and 6.25) filling the dielectric hole, as shown in figure 2(a). For simplicity of calculation, the unit cell is chosen as one of an array of silver nanobeads (see figure 1(a)). On the surface of the outer simulation region we set periodic boundary condition along the side walls and the PML condition on the top and bottom surface. The period of the unit cells is set to be $P = 400$ nm.

It can be observed from figure 2(a) that only one dip is present in the cases of $\varepsilon = 1$ (at $\lambda = 525$ nm) and $\varepsilon = 3$ (at $\lambda = 600$ nm), and two dips are present in the case of $\varepsilon = 6.25$ (at $\lambda = 400$ and 725 nm). These two resonances modes are associated with the bonding and anti-bonding modes that can be explained by the plasmonic hybridization model [22–31].

The cylindrical dielectric core in a nanobead can be considered as a truncated circular waveguide. The value of near field intensity strongly depends on the medium filling the dielectric holes, the thickness of the nanometal and the interparticle spacing [6]. A medium with a higher dielectric constant inside the dielectric holes makes the effective size of the dielectric hole increase and increases the effective refractive index n_{eff} [15]. As shown in figure 2(a), when the dielectric constant of the medium inside the dielectric holes varies from $\varepsilon = 1$ to 3, the dip is shallower and the position of the dip is toward a higher wavelength (it is red-shifted). For the case of $\varepsilon = 1$, a clear dip with respect to a bonding plasmon resonance mode (we name it 'mode I' hereafter) can be found at $\lambda = 525$ nm. As the permittivity of the dielectric hole is increased to a higher value of $\varepsilon = 6.25$, a sharper dip relating to an anti-bonding plasmon resonance mode (we name it 'mode II' hereafter) occurs at $\lambda = 400$ nm, and a weaker bonding plasmon resonance mode (mode I) appears at $\lambda = 725$ nm. Therefore, both the bonding and anti-bonding modes can be found for cores with higher indices filling the dielectric hole. Three mode Is and one mode II can be seen in figure 2(a).

In order to determine the mechanism of the above phenomena, the selective corresponding plasmon resonance modes and their near field distributions are also depicted. Figures 2(b) and (c) show the electric field distribution and propagation (white arrows) in the case of $\varepsilon = 6.25$ corresponding to mode I and mode II, respectively. The optical response of the mode I case is quite different from that of the mode II case. In mode II ($\lambda = 400$ nm), we

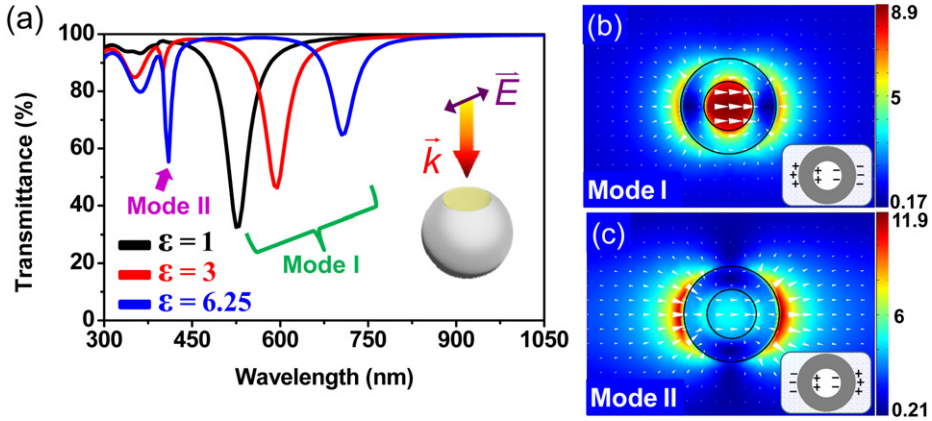

Figure 2. (a) Difference in transmittance spectra on an array of silver nanobeads with media of different dielectric constants ($\varepsilon = 1$, 3 and 6.25) inside the dielectric hole. Electric field distribution and propagation (white arrows) in the case $\varepsilon = 6.25$ corresponding to (b) mode I and (c) mode II, respectively.

observe that the intensity of the electric field along the polarization direction occurring at the two outer surfaces of the silver nanobead is stronger than that inside the nanobead (the dielectric core region). On the contrary, in mode I ($\lambda = 725$ nm) the stronger electric field exists in the dielectric region. These large plasmon resonant local field enhancements are similar in magnitude to the localized plasmon resonant 'hot spots' occurring at junctions between metallic nanoparticles when a dimer plasmon resonance is excited [15, 22]. The nanobead local fields should give rise to intense surface-enhanced Raman scattering (SERS) enhancements with the added advantage that the hot spots are completely open to the surrounding medium in this geometry. From this point of view, each nanobead particle can potentially serve as a standalone, optically addressable nanoscale substrate for surface-enhanced spectroscopies.

Regarding the direction of electric field propagation (white arrows), the schematic charge distributions of mode I and mode II are also depicted in the inset of figures 2(b) and (c), respectively. In mode I (see the inset of figure 2(b)), the distributed charges on the inner and outer surfaces of the nanobead are the same, resulting in bonding mode resonance. Turning to mode II (see the inset of figure 2(c)), the distributed charges on the inner and outer surfaces of the nanobead are dipole-like, leading to an anti-bonding mode resonance. As a result, the radiation loss in the anti-bonding resonance mode case is suppressed, which shows a sharper transmittance dip than the bonding mode resonance case. The resonant wavelengths for both mode I and mode II are shifted to the longer wavelength as the dielectric constant of the filling increased.

It is worth emphasizing here that the anti-bonding mode resonance is hardly excited by the illumination of a plane wave. As mentioned in other research, to excite the anti-bonding mode resonance, the symmetry of the geometric structure needs to be broken [23]. Besides breaking the symmetry of the structure, the anti-bonding mode can be excited under asymmetric illumination, such as by a localized source [32], total internal reflection [33], and a displaced focused laser beam [34]. In addition, we found that it is possible to excite the anti-bonding mode by breaking the geometric symmetry of structures directly, i.e. by varying the medium filling the dielectric hole. According to the simulation results of figure 2(c), the symmetry can be broken by filling a nanobead with a dielectric core, resulting in both bonding and anti-bonding resonance modes.

Now, we investigate the case of a nanobead dimer (see figure 1(b); the unit cell is formed by two silver nanobeads). Figure 3(a) shows the transmittance spectra of a silver nanobead dimer with three different media filling the dielectric holes. The dimensions of a nanobead within a silver nanobead dimer are the same as in figure 2(a). Comparing the results obtained from figure 2(a) with figure 3(a) shows that the dips in figure 3(a) are much deeper than those of figure 2(a), and are red-shifted toward higher wavelengths. As mentioned above, the anti-bonding mode can be excited by breaking the symmetry as the dielectric constant of the medium filling the dielectric hole is increased. Figures 3(b) and (c) show the electric field distribution and propagation (white arrows) corresponding to mode I and mode II, respectively. Because of coupling effects between two silver nanobeads, we find that the electric field is enhanced and forms a hot spot in the gap for both mode I and mode II, and the electric field is suppressed elsewhere, which shows quite a different pattern from the results obtained in figures 2(b) and (c).

The field distributions can help us to understand how the light is distributed through the silver nanobead dimer. To realize the detailed behavior of the field distribution around a silver nanobead pair, figures 4(a) and (b) show the near field intensity versus three different refractive indices of dielectric holes along the x axis (shown in the inset of figure 4) in the range of $x = [-150, 150]$ nm corresponding to mode I and mode II, respectively.

As shown in figures 4(a) and (b), an opposite result is found in the gap of the silver nanobead dimer, i.e. a filling with a higher dielectric constant results in a lower gap enhancement for mode I. For mode II, the situation is reversed. In addition,

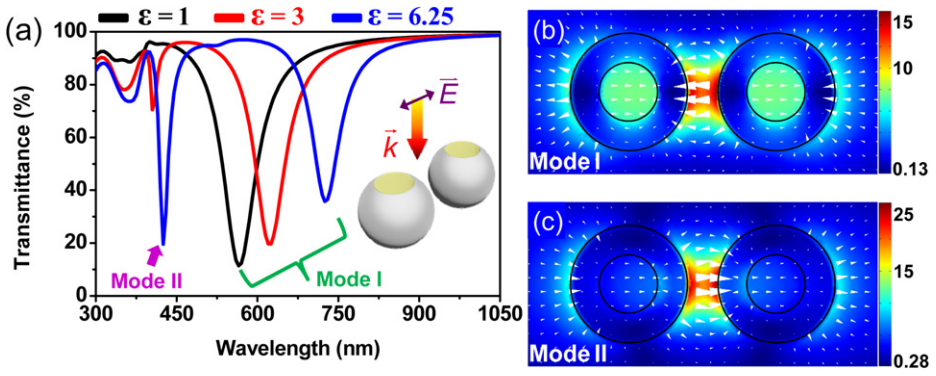

Figure 3. (a) Transmittance spectra of a silver nanobead dimer with three different media filling the dielectric hole. The dimensions of a nanobead within a silver nanobead dimer are same as in figure 2(a). Electric field distribution and propagation (white arrows) corresponding to (b) mode I and (c) mode II, respectively.

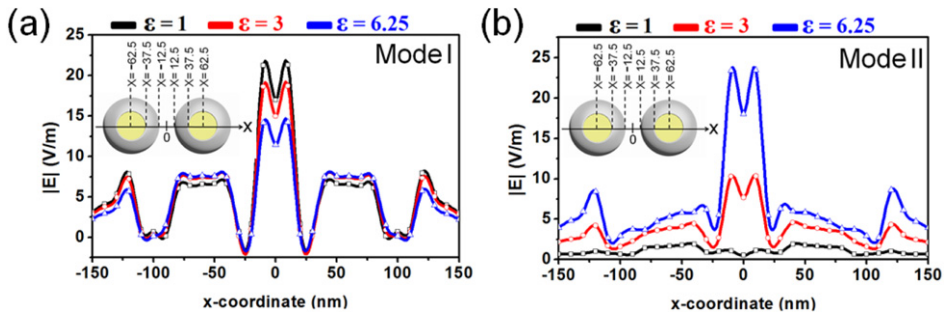

Figure 4. Near field intensity versus three different refractive indices of dielectric holes along the x axis (at $y = 0$, shown in the inset) in the range of $x = [-150, 150]$ nm corresponding to mode I and mode II, respectively.

the near field intensity of mode II (anti-bonding mode) is more sensitive than that of mode I (bonding mode) to the various media inside the dielectric hole.

For the medium filling the dielectric hole, we show how the silver nanobead resonance varies with the medium comprising the core while the overall particle size and aspect ratio of the nanoparticle are held constant, for mode I and mode II resonances of the nanostructure. As the core index decreases (e.g. $\varepsilon = 1$ and 3), the hybridization between the cavity and spheroid modes becomes progressively stronger, resulting in larger energy gaps between the bonding and anti-bonding plasmon modes [22]. The 'bonding' plasmon modes of the nanobeads are more sensitive to the core and shell dimensions than the 'anti-bonding' plasmon modes. The nanobead plasmon modes significantly increase the geometrically and materially sensitive hybrid plasmon resonances by varying the core indices and can be tuned across a broader spectral range than the parent solid spheroid and cavity plasmon modes. The near field intensity and transmittance spectrum can be tuned by varying the index of the core inside the nanobead dimer. Such environmental sensitivity of the nanobead plasmons holds great potential for monitoring local environmental changes during chemical and biological processes and switchable plasmonic devices. For example, it is possible to tune and shift the optical responses of the nanobead system by filling 'phase change materials' (with a dielectric constant that can be switched through modulation of the input energy for phase transition between amorphous and crystalline phase states [35–39]) inside the silver nanobeads.

4. Conclusion

In summary, we numerically investigate the plasmonic resonance mode and coupling effect of single silver nanobeads and silver nanobead dimers. Numerical investigation using 3D FEM indicates that the silver nanobead exhibits two plasmonic resonances corresponding to bonding and anti-bonding modes, respectively. The boundary symmetry at the inner and outer surfaces of the silver nanobead can be broken by increasing the refractive indices of the cores inside the dielectric holes. On the basis of our simulations, it is shown that the bonding mode can be found at lower core dielectric constants (e.g. $\varepsilon = 1$ and 3) and both the bonding and anti-bonding modes can be found at higher core dielectric constants (e.g. $\varepsilon = 6.25$). It is possible to excite the anti-bonding by breaking the geometric symmetry of structures directly, i.e. by varying the medium filling the dielectric hole. This unique properties of a silver nanobead or a silver nanobead dimer are highly attractive for serving as resonant nanocavity to hold and probe smaller nanostructures, such as biomolecules or quantum dots. Nanobeads also show significant promise for applications in nano-switch devices, sensing, and surface-enhanced spectroscopy, due to their strong and tunable plasmon resonances.

Acknowledgments

The authors acknowledge financial support from National Science Council, Taiwan, under grant numbers 99-M-2112-231-001-MY3, 100-2923-M-002-007-MY3, NSC 101-3113-P-002-021-, and NSC 101-2112-M-002-023-. We are also grateful to the National Center for Theoretical Sciences, Taipei Office, Molecular Imaging Center of National Taiwan University, National Center for High-Performance Computing and Research Center for Applied Sciences, Academia Sinica, Taiwan, for their support.

References

[1] Homola J, Yee S S and Gauglitz G 1999 Surface plasmon resonance sensors: review *Sensors Actuators* B **54** 3–15
[2] Peng T C, Lin W C, Chen C W and Tsai D P 2011 Enhanced sensitivity of surface plasmon resonance phase-interrogation biosensor by using silver nanoparticles *Plasmonics* **6** 29–34
[3] Bergman D J and Stockman M I 2003 Surface plasmon amplification by stimulated emission of radiation: quantum generation of coherent surface plasmons in nanosystems *Phys. Rev. Lett.* **90** 027402
[4] Zheludev N I, Prosvirnin S L, Papasimakis N and Fedotov V A 2008 Lasing spaser *Nature Photon.* **2** 351–4
[5] Plum E, Fedotov V A, Tsai D P and Zheludev N I 2009 Towards the lasing spaser: controlling metamaterial optical response with semiconductor quantum dots *Opt. Express* **17** 8548–51
[6] Chen W T, Wu P C, Chen C J, Weng C J, Lee H C, Yen T J, Kuan C H, Mansuripur M and Tsai D P 2011 Manipulation of multidimensional plsamonic spectra for information storage *Appl. Phys. Lett.* **98** 171106
[7] Chen W T, Chen C J, Wu P C, Sun S, Zhou L, Guo G Y, Hsiao C T, Yang K Y, Zheludev N I and Tsai D P 2011 Optical magnetic response in three-dimensional metamaterial of upright plasmonic meta-molecules *Opt. Express* **19** 12837–42
[8] Huang Y W, Chen W T, Wu P C, Fedotov V, Savinov V, Ho Y Z, Chau Y F, Zheludev N I and Tsai D P 2012 Design of plasmonic toroidal metamaterials at optical frequencies *Opt. Express* **20** 1760–8
[9] Tsai D P, Kovacs J, Wang Z H, Moskovits M, Shalaev V M, Suh J S and Botet R 1994 Photon scanning-tunning-microscopy images of optical-excitations of fractal metal colloid clusters *Phys. Rev. Lett.* **72** 4149–52
[10] Barnes W L, Dereux A and Ebbesen T W 2003 Surface plasmon subwavelength optics *Nature* **424** 824–30
[11] Liu W C and Tsai D P 2002 Optical tunneling effect of surface plasmon polaritons and localized surface plasmon resonance *Phys. Rev.* B **65** 155423
[12] Miller M M and Lazarides A A 2006 Sensitivity of metal nanoparticle plasmon resonance band position to the dielectric environment as observed in scattering *J. Opt. A: Pure Appl. Opt.* **8** S239
[13] Xu S, Cao Y C, Zhou J, Wang X, Wang X and Xu W 2011 Plasmonic enhancement of fluorescence on silver nanoparticle films *Nanotechnology* **22** 275715
[14] Kelly K L, Coronado E, Zhao L L and Schatz G C 2003 The optical properties of metal nanoparticles: the influence of size, shape, and dielectric environment *J. Phys. Chem.* B **107** 668–77
[15] Chau Y F, Yeh H H and Tsai D P 2008 Near-field optical properties and surface plasmon effects generated by a dielectric hole in a silver-shell nanocylinder pair *Appl. Opt.* **47** 5557–61
[16] Chau Y F, Lin Y J and Tsai D P 2010 Enhanced surface plasmon resonance based on the silver nanoshells connected by the nanobars *Opt. Express* **18** 3510–8
[17] Chau Y F, Yeh H H, Liao C C, Ho H F, Liu C Y and Tsai D P 2010 Controlling surface plasmon of several pair arrays of silver-shell nanocylinders *Appl. Opt.* **49** 1163–9
[18] Chau Y F, Sun Y S, Tsai D P and Yang T J 2007 The optical properties between an incident wave and the active layer of a bubble-pit AgOx-type super-resolution near-field structure *Appl. Phys.* A **89** 381–5
[19] Kottmann J P, Martin O J F, Smith D R and Schultz S 2000 Spectral response of plasmon resonant nanoparticles with a non-regular shape *Opt. Express* **6** 213–9
[20] Chen X W, Choy C H, He S and Chiu P C 2007 Highly efficient fluorescence of a fluorescing nanoparticle with a silver shell *Opt. Express* **15** 7083–94
[21] Rakic A D, Djurisic A B, Elazar J M and Majewski M L 1988 Optical properties of metallic films for vertical-cavity optoelectronic devices *Appl. Opt.* **37** 5271–83
[22] Prodan E, Radloff C, Halas N J and Nordlander P 2003 A hybridization model for the plasmon response of complex nanostructures *Science* **302** 419–22
[23] Hao F, Sonnefraud Y, Van Dorpe P, Maier S A, Halas N J and Nordlander P 2008 Symmetry breaking in plasmonic nanocavities: subradiant LSPR sensing and a tunable fano resonance *Nano Lett.* **8** 3983–8
[24] Halas N 2002 The optical properties of nanoshells *Opt. Photon. News* **13** 26–30
[25] Prodan E, Lee Allen and Nordlander P 2002 The effect of a dielectric core and embedding medium on the polarizability of metallic nanoshells *Chem. Phys. Lett.* **360** 325–32
[26] Prodan E, Nordlander P and Halas N J 2003 Effects of dielectric screening on the optical properties of metallic nanoshells *Chem. Phys. Lett.* **368** 94–101
[27] Prodan E, Nordlander P and Halas N J 2003 Electronic structure and optical properties of gold nanoshells *Nano Lett.* **3** 1411–5
[28] Hao E, Li S, Bailey Ryan C, Zou S, Schatz George C and Hupp Joseph T 2004 Optical properties of metal nanoshells *J. Phys. Chem.* B **108** 1224–9
[29] Tam F, Moran C and Halas Naomi J 2004 Geometrical parameters controlling sensitivity of nanoshell plasmon resonances to changes in dielectric environment *J. Phys. Chem.* B **108** 17290–4
[30] Radloff C and Halas Naomi J 2004 Plasmonic properties of concentric nanoshells *Nano Lett.* **4** 1323–7
[31] Prodan E and Nordlander P 2004 Plasmon hybridization in spherical nanoparticles *J. Chem. Phys.* **120** 5444–54
[32] Liu M, Lee T-W, Gray S K, Guyot-Sionnest P and Pelton M 2009 Excitation of dark plasmons in metal nanoparticles by a localized emitter *Phys. Rev. Lett.* **102** 107401
[33] Yang S-C, Kobori H, He C-L, Lin M-H, Chen H-Y, Li C, Kanehara M, Teranishi T and Gwo S 2010 Plasmon hybridization in individual gold nanocrystal dimers: direct observation of bright and dark modes *Nano Lett.* **10** 632–7
[34] Huang J-S, Kern J, Geisler P, Weinmann P, Kamp M, Forchel A, Biagioni P and Hecht B 2010 Mode imaging and selection in strongly coupled nanoantennas *Nano Lett.* **10** 2105–10
[35] Samson Z L, MacDonald K F, De Angelis F, Gholipour B, Knight K, Huang C C, Di Fabrizio E, Hewak D W and Zheludev N I 2010 Metamaterial electro-optic switch of nanoscale thickness *Appl. Phys. Lett.* **96** 143105
[36] Samson Z L, Yen S-C, MacDonald K F, Knight K, Li S, Hewak D W, Tsai D P and Zheludev N I 2010

Chalcogenide glasses in active plasmonics *Phys. Status Solidi (RRL)* **4** 274–6

[37] Chiu K P, Lai K F and Tsai D P 2008 Application of surface polariton coupling between nano recording marks to optical data storage *Opt. Express* **16** 13885–92

[38] Chang C M, Chu C H, Tseng M L, Chiang H-P, Mansuripur M and Tsai D P 2011 Local electrical characterization of laser-recorded phase-change marks on amorphous $Ge_2Sb_2Te_5$ thin films *Opt. Express* **19** 9492–504

[39] Tseng M L, Chen B H, Chu C H, Chang C M, Lin W C, Chu N-N, Mansuripur M, Liu A Q and Tsai D P 2011 Fabrication of phase-change chalcogenide $Ge_2Sb_2Te_5$ patterns by laser-induced forward transfer *Opt. Express* **19** 16975–84